Analytical Methods

Accepted Manuscript

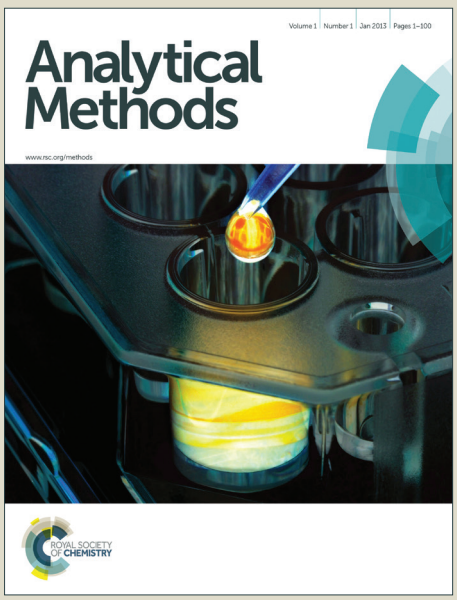

ROYAL SOCIETY OF CHEMISTRY

www.rsc.org/methods

Journal Name

ARTICLE

A molecularly imprinted electrochemical sensor based on gold nanoparticle/carbon nanotube hybrids material for sensitive detection of isoniazid

Received 00th January 20xx,
Accepted 00th January 20xx

DOI: 10.1039/x0xx00000x

www.rsc.org/

Bowan Wu, Lijie Hou, Tiantian Zhang, Yanxia Han and Chao Kong

Molecular imprinted technique (MIT) is an approach to synthesize a polymer matrix with molecular recognition sites, which shows specific binding behaviors to target molecule. MIT has been successfully applied in sensing areas due to their mechanical and chemical stability, high affinity and outstanding substrate recognition ability, low cost and easy preparation. Based on gold nanoparticles/carbon nanotubes hybrids material(AuNP-CNT) and molecularly imprinted polymer (MIP), we propose a novel molecularly imprinted electrochemical sensor to determine isoniazid (INH) selectively. The surface of glassy carbon electrodes(GCE) are modified by multi-walled carbon nanotubes (MCNT) decorated with gold nanoparticles (AuNP). The selectivity of INH detection is improved by MIP membrane, and the area of electrochemistry active surface area is increased by AuNP-MCNT nanometer complex. INH is detected by stripping voltammetry and the effect sound. The oxidation peak current and INH concentration have linear relationship in range of 1×10^{-9} to 1.4×10^{-8} M and 2×10^{-8} to 1.0×10^{-7} M, resepectively. The detection limit is 0.3×10^{-9}M (3σ) INH with relative standard deviation 4.6% (n=8) for 5×10^{-8}M INH after 60s enrichment. The sensor can be applied to detect the INH in body fluid and pharmaceutical samples selectively. The solution of MIP AuNP–MCNT/GCE exhibits remarkable advantages, such as low cost, easy to use, high selectivity and sensitivity.

Introduction

Isoniazid (isonicotinoylhydrazine, INH) is widely used for clinical purposes as a tuberculostatic agent effective to restrain mycobacterium strains [1]. The drug action mechanisms proposed show that the bacteriostatic or bacteriocidal action of isoniazid is achieved by interfering the metabolism of bacterial proteins, nucleic acids, carbohydrates and lipids.[2]. But the poisoning accidents and death happened occasionally due to overdosage of isoniazid[3-6]. Therefore, the control of the isoniazid dose for sufferers is very important in clinical chemistry.

The determination methods of INH have been developed due to its importance [7], including titrimetry[8, 9], colorimetric[10], spectrophotometry[11], fluorimetry[12-14], high performance liquid chromatography[15-18], capillary electrophoresis[19, 20], chromatographic[21], chemiluminescence[22-25], electrochemiluminescence[26, 27], the chemometric methods[28, 29], and electroanalytical methods [30-37]. Among these approaches, electroanalytical techniques have particular advantage because of their practicality, simplicity, low-cost, good sensitivity, precision and rapidity for real-time detection. In electroanalytical area, the concept of chemically modified electrodes has been developed to repalce conventional electrodes for improving the reactivity, sensitivity and selectivity of the electrode reactions in many applications. Various types of modified electrodes have also been used to detect isoniazid[37, 38]. But in most cases, the oxidation of isoniazid at aforementioned modified electrodes always require a high overpotential and a non-neutrality supporting electrolyte, which brings great inconvenience to the analytical procedure, and are unsuitable for the on site detection. Hence, it is required imminently to find a sensitive modified electrode which could decrease the overpotential of isoniazid oxidation and detect isoniazid in neutral media simultaneously.

Carbon nanotubes (CNT)[39] are ideal materials for incorporation into electrochemical sensors due to their high surface area, high aspect ratio, and enhanced catalytic properties. Accordingly, researchers continue to develop novel uses for these nanomaterials in electrochemical sensors at a rapid pace [40-44]. It has been reported that the small size of gold nanoparticles (AuNP) allow the conductive materials to come into the vicinity of the active process providing bioelectrocatalytic activity that can be utilized in the construction of biosensors [45]. AuNP are being increasingly used in

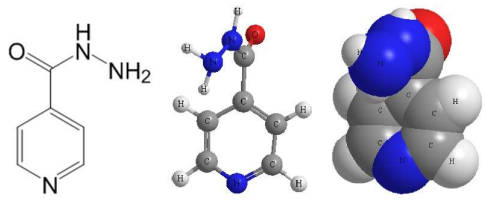

Fig. 1 Structural of INH(Chemical structural, Ball & stick model, space-filling model)

LONGDONG UNIVERSITY-FLUOBON Surfactant Engineering Technology Center, College of Chemistry & Chemical Engineering, Cooperative Innovation Center of Industrial Surfactant, Longdong University, 45 Lanzhou Road, Qingyang, China.
E-mail: bowanwu@ldxy.edu.cn; Fax: +86-934-8651531; Tel: +86-15701709818

many electrochemical applications due to its ability in enhancing the electrode conductivity and facilitating the electron transfer[46-48]. More recently, the CNT & metallic nanocomposites has attracted much interest in the construction of electrochemical sensors because of the low resistance ohmic contacts of these composites [49, 50]. Of particular interest are nanocomposites involving AuNP due to the combination of the unique electronic properties of CNT and their ease of surface modification, along with the biocompatibility and electrocatalytic effects of AuNP [51-54].

Molecularly imprinted polymer (MIP) has been applied in chemical sensing area[55]. Different types of MIP nanosensor has been reported in the literatures[56-58], such as quartz crystal microbalance (QCM) nanosensor[59-62] and surface plasmon resonance (SPR) biosensor[63-65].

In this study, an AuNP decorated MCNT modified glassy carbon electrode (AuNP–MCNT/GCE) was fabricated for the determination of INH. At the modified electrode, remarkable peak current enhancement of INH occurred compared with that of the bare GCE and the MCNT modified glassy carbon electrode (MCNT/GCE). The AuNP–MCNT hybrid exhibit remarkable ability to increase the electroactive surface area and promote the electron-transfer rate between the electrode and the analyte. Consequently, an adsorptive stripping voltammetry method based on the AuNP–MCNT/GCE was developed for the determination of INH concentration. The electrochemical sensor can be used for determination of concentration of INH in pharmaceutical assays. After that a sensitive and rapid electrochemical method was developed for detecting the concentration of INH. The oxidation peak current changes linearly with the concentration of INH in the range from 1×10^{-9} to 1.4×10^{-8}mol/L and 2×10^{-8} to 1.0×10^{-7} mol/L, separately. The detection limit is about 0.3×10^{-9}mol/L for 60 s accumulation. The relative standard deviation is 4. 6% for 5×10^{-8}mol/L INH (n=8). Finally, this method was successfully employed to determine INH in INH tablets and blood serum.

Experimental

Reagents and instruments

MCNT with diameter of 20-40nm was purchased from Shenzhen Nanotech Port Co., Ltd. $HAuCl_4\cdot4H_2O$ was purchased from Shanghai Chemical Factory. Nafion solution (DE520, 5% in ethanol) was purchased from DuPont Co. Isoniazid (INH) was purchased from Aladdin Chemistry Co. Ltd. Other chemicals were analytical grade and used without further purification. Doubly distilled water and high-purity N_2 were used. All experiments were carried out at ambient temperature.

Apparatus

Electrochemical measurements were carried out on a CHI832 electrochemical workstation (ChenHua Instruments Co., Shanghai, China) with a conventional three electrode system comprising platinum wire as auxiliary electrode, saturated calomel electrode (SCE) as reference and the bare electrode or modified glass carbon electrode (GCE) as working electrode. Electrochemical impedance spectroscopy (EIS) experiments were performed on a VMP2 Multi-potentiostat (Princeton Applied Research, USA), which was controlled by EC-Lab (V9.24) software (Bio- Logic SA). The surface morphologies of the modified electrodes were observed through scanning electron microscopy (SEM) on JSM-6701F (Japan Electron Optics Company). Scanning electron microscopy (SEM) images were collected on a Hitachi s-4800 field emission scanning electron microscope (Japan). The pH measurements were performed with PB-10 pH meter (Sartorius, Germany).

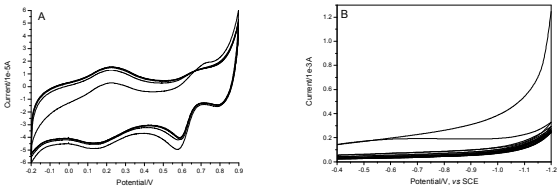

Fig. 2(A) CV for the electrodeposition of AuNP on MCNT-GCE in 0.2M K_2SO_4 solution containing 1mM $HAuCl_4$ from -0.2 to 1.0V with a scan rate of 50mV/s. Fig. 2(B) CV for the electropolymerization MIP in 2.0×10^{-3}mol/L acrylamide and 1.6×10^{-3}mol/L N,N'-methylene diacrylamide on AuNP-MCNT-GCE with a scan rate of 10mV/s.

Preparation of the MIP AuNP–MCNT/GCE

Prior to modification, the GCE was polished with 0.3 and 0.05μm alumina slurry and rinsed thoroughly with doubly distilled water between each polishing step. Then, it was washed successively with 1:1 nitric acid, acetone and doubly distilled water in an ultrasonic bath and dried in air.

The commercially available MCNT was dispersed in a 1:3 (V/V) mixture of concentrated HNO_3 and H_2SO_4 in a 100 mL flask at room temperature with continuous ultrasonication for 2 h, and then heated at 80 ℃ in an oil bath with reflux condenser and vigorous magnetic stirring for 12h. Subsequently, the product was centrifuged, filtered, and washed up to neutral pH. Finally, the sample was dried under vacuum at 50 ℃ overnight. 1.0 mg of the treated MCNT was dispersed in 5mL of Nafion solution (0.5%) and ultrasonicated for 30 min until a homogenous suspension of MCNT was obtained. Then, 5μL MCNT suspension was carefully casted on the surface of well-polished GCE and dried by infrared lamp. Thus the MCNT/GCE electrode was obtained.

Then, the MCNT/GCE electrode was immersed in 0.2M K_2SO_4 solution containing 1mM $HAuCl_4$. The electrodeposition of AuNP onto MCNT/GCE was conducted by CV scanning from 0.2 to -1.0V with a scan rate of 50 mV/s for 10 cycles. The AuNP–MCNT/GCE was taken out and rinsed with deionized water. Finally, the modified electrode was activated by several successive potential scans from 0.4 to 1.0V with a scan rate of 50 mV/s in phosphate buffer solutions (PBS) (pH 7.4) until a steady voltammogram was obtained.

The INH MIP membrane was fabricated through the electrochemical copolymerization[66]. The electropolymerization was performed by CV (10 cycles) in the potential range of -1.2 to -0.4V with a scan rate of 10mV/s in 0.2M $NaNO_3$ electrolyte solutions containing 2.0×10^{-3}mol/L acrylamide(functional monomer), 1.6×10^{-3}mol/L N,N'-methylene diacrylamide (crosslinking agent), 1mg ammonium persulfate (catalyst) and 2.0×10^{-4}M INH (template) in pH=13.5 after bubbling high-purity nitrogen for at least 10 min to remove dissolved oxygen, as show in Fig. 2(B). Similarly, the non-

MIP was also fabricated in the absence of INH. Then, MIP electrode was activated and removed the INH template by several successive potential scans from 0 to 1.0V with a scan rate of 50 mV s^{-1} in PBS (pH 7.4) until a steady voltammogram was obtained. The overall process of INH MIP AuNP-MWCNT/GCE sensor fabrication was summarized in Scheme 1.

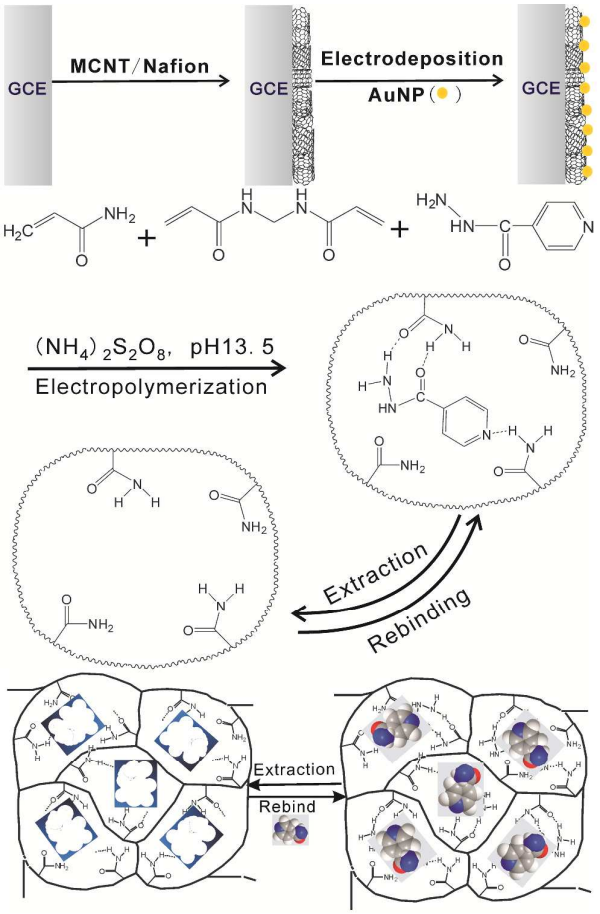

Scheme 1. Schematic of INH MIP AuNP-MCNT/GCE fabrication process

Results and discussion

Morphological characterization of the AuNP–MCNT/GCE

The surface morphology of the AuNP–MCNT/GCE was characterized by SEM. As shown in Fig. 3A, We can see clearly the diameter of the MCNT was about 30 nm, which would benefit the sensor performance [67, 68]. In Fig 3B, a network-like structure of MCNT was observed on surface of electrode surface, which indicated that the MCNT were immobilized on the GCE surface. Fig 3C indicated that AuNP electrodeposited on the MCNT were spherical with an average diameter about 30-50nm and well distributed. The rough surface provided a large surface area for adsorbing the target molecular.

Electrochemical characterization of the AuNP–MCNT/GCE

Cyclic voltammetry (CV) was employed to characterize the characteristic peak of Au. CV of 0.5M H_2SO_4 solution on bare GCE (a), MCNT/GCE (b) and AuNP–MCNT/GCE (c) are shown in Fig.4. In curve (b) of Fig. 4, there is no obvious redox peak on MCNT/GCE. However, there are similar redox peaks on bare Au (Fig 4a) and AuNP–MCNT/GCE (Fig 4c), indicating that AuNP were successfully decorated on the surface of MCNT/GCE[69]. Especially, the peak curent of AuNP–MCNT/GCE much higher than bare Au, that is ascribe to the larger electrochemical activity surface of AuNP.

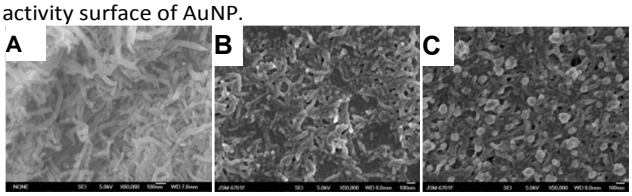

Fig. 3 SEM images of (A) MCNT, (B) MCNT-Nafion, (C) AuNP-MCNT/GCE

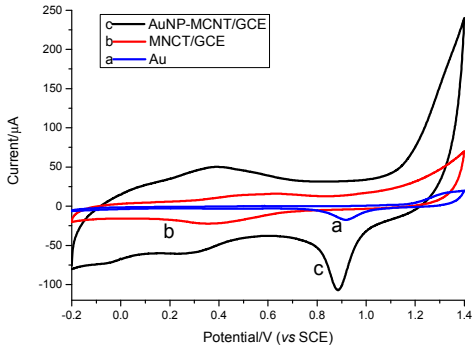

Fig. 4 CVs of the(a)bare Au, (b)MCNT/GCE, (c)AuNP–MCNT/GCE in 0.5M H_2SO_4 with a scan rate of 50 mV/s

CV and EIS experiments were used to characterize the AuNP–MCNT/GCE. CVs of 5.0mM $Fe(CN)_6^{3-/4-}$ containing 0.2M KCl solution on bare GCE (a), MCNT/GCE (b) and AuNP–MCNT/GCE (c) are shown in Fig. 5A. The quasi-reversible one-electron redox behavior of ferricyanide ions was observed on the bare GCE at the scan rate of 50mV/s. After being modified with MCNTs, the peak current of $Fe(CN)_6^{3-/4-}$ was increased. For the deposition of AuNP on the MCNT/GCE, the peak current of $Fe(CN)_6^{3-/4-}$ was further increased compared with that of the MCNT/GCE, indicating that the introduction of the AuNP–MCNT hybrid played an important role in the increase of the electroactive surface area and provided the conducting bridges for the electron-transfer of $Fe(CN)_6^{3-/4-}$.

EIS is also an efficient tool for studying the interface properties of surface-modified electrodes. The electron-transfer resistance (Rct) at the electrode surface is equal to the semicircle diameter of EIS and can be used to describe the interface properties of the electrode. Fig. 5B indicates the results for the impedance spectrum on bare GCE (a), MCNT/GCE (b) and AuNP–MCNT/GCE (c). The measurements in this work were carried out in a background solution of 5.0mM Fe(CN)63−/4− in the presence of 0.2M KCl. The R(C(RW)) equivalent circuit model (inset of Fig. 5B) was chosen to fit the obtained impedance data containing the electron transfer process (modeled as a resistance to charge transfer,

Rct) and the diffusion process (modeled as the Warburg-type impedance, W). The Rct and W were both in parallel with the interfacial capacitance (Cdl). The diameter of the semicircle corresponds to the interfacial electrontransfer resistance (Rct) [70, 71]. By fitting the data, Rct was estimated to be 248 Ohm at the bare GCE (a), while the Rct decreased to 95 Ohm due to the accelerating of electron-transfer rate by MCNTs (b), and

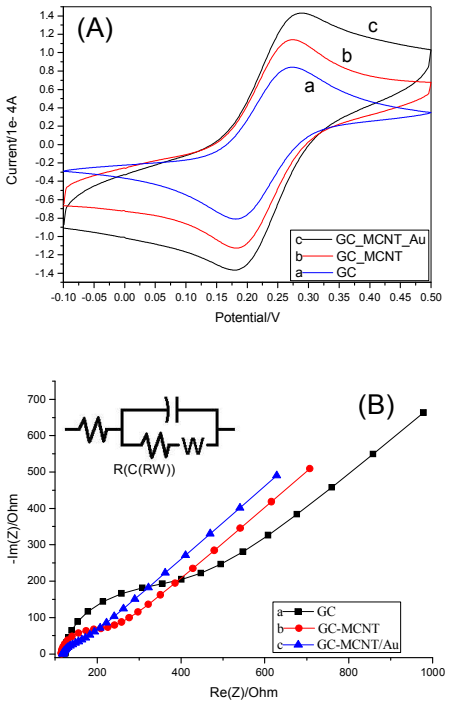

Fig. 5. (A) CVs of 5.0mM $Fe(CN)_6^{3-/4-}$ containing 0.2M KCl solution on a bare GCE (a), a MCNT/GCE (b) and an AuNP–MCNT/GCE (c). (B) Nyquist plots of 5.0mM $Fe(CN)_6^{3-/4-}$ containing 0.2M KCl solution with a bare GCE (a), a CNT/GCE (b) and an AuNP–CNT/GCE (c). The frequency range is from 100mHz to 100 kHz. Inset is the equivalent circuit.

the Rct decreased to 29 Ohm With the AuNP–MCNT/GCE(c), revealing the much lower electron-transfer resistance on the AuNP–MCNT/GCE compared with MCNT/GCE. The results were consistent with the CV results. All of these results demonstrates that AuNP–MCNT nanohybrid might provide higher electron conduction pathways due to the synergistic effect[72].

The response of INH on the AuNP–MCNT/GCE

CV was utilized to investigate the electrochemical behavior of 50nM INH in PBS (pH6.8) with bare GCE, CNT/GCE and AuNP–MCNT/GCE (Fig 6A). In Fig 6A, there is no obvious oxidation peak on the bare GCE and bare Au electrode in the potential range from 0 to 0.8V. However, one oxidation peak at 0.366V was observed on the MCNT/GCE, and two oxidation peaks at 0.333V and 0.58V were observed on the Au-MCNT/GCE, revealing that INH underwent an irreversible oxidation-reduction process on MCNT/GCE and AuNP-MCNT/GCE. We can see clearly that the oxidation peak current of MCNT/GCE was 6 times higher compared with bare GCE, which can be related to the high conductivity and big specific surface area of MCNT. On the AuNP-MCNT/GCE, the INH oxidation potential was decreased to 0.333V, which was a further decrease of 0.033V compared to the MCNT/GCE. Furthermore, the extra 1.8-fold increase in the peak current can be associated with the more efficient catalytic effect of AuNP in INH oxidation. These phenomena demonstrated that the AuNP-MCNT hybrid could efficiently accelerate the electron-transfer at the electrode surface and improve the electrochemical performance accordingly. To better understand the reaction mechanism of INH, the linear sweep voltammetry was employed to examine the relation between different scan rate and peak current on AuNP–MCNT/GCE (Fig 6B). Fig. 6B illustrates that the oxidation peak currents of INH are proportional to the scan rate in the range of 10-50mV/s in the PBS (pH 7.4), indicating a surface absorption-controlled process at low sweep rate. However, the oxidation peak currents of INH were proportional to the square root of the scan rate in the range of 60-200mV/s, $i_p(A) = 6.6291\times10^{-5} + 4.3497\times10^{-7}\ v^{1/2}$ $(V/s)^{1/2}$ (r = 0.9983) (Fig 6C), indicating a diffusion-controlled process at high sweep rate. These results indicate that the oxidation process of INH includes two electrons and two protons, and the reaction mechanism is same with the oxidation of amino[31, 73]. At the process of measurements by linear sweep voltammetry, while the sweep rate was too fast, the faraday double-layer capacitance charging current and ohmic potential drop of solution would severely influence the experiment results. Conversely, while the sweep rate was too low, the low current would decrease the sensitivity of biosensor. For the above reasons, 50mV/s was the suitable sweep rate in our experiment.

Optimizing the performance of MIP AuNP–MCNT/GCE sensor

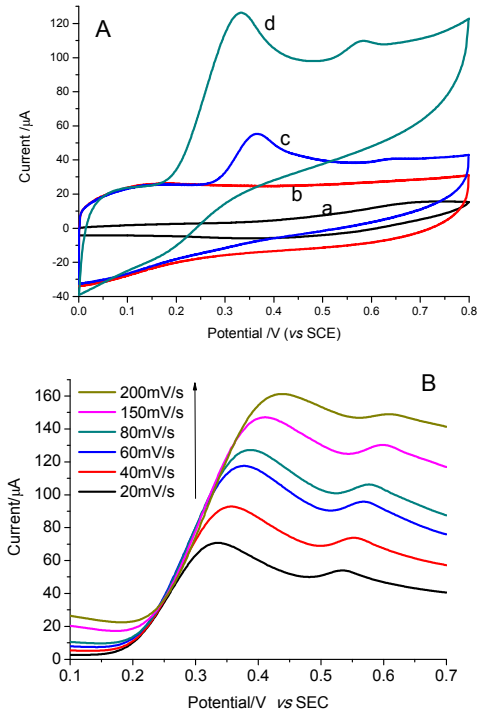

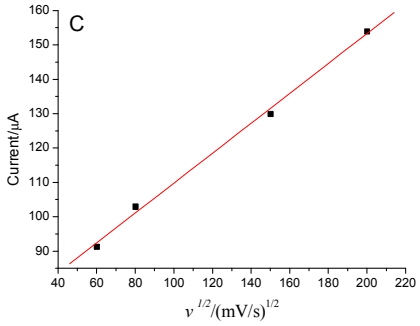

Fig. 6. (A) CVs of bare GCE (a), bare Au(b), MCNT/GCE (c) and AuNP–MCNT/GCE (d) in 0.1M PBS (pH 6.8) containing 50nM INH, with a scan rate of 50 mV/s. (B) LSSV of AuNP–MCNT/GCE in 0.1M PBS (pH 6.8) containing 50nM INH with different scan rates. (C)The oxidation peak currents of INH to the square root of the scan rate in the range of 60-200mV/s.

The effect of the supporting electrolytes on voltammograms of INH was investigated, which included 0.1 M HAc-NaAc, 0.1 M PBS, 0.1 M NH_3-NH_4Cl and 0.1 M Britton-Robinson. The experimental results showed that the oxidation peak of INH could be obtained in all the above electrolytes. However, in PBS (pH 6.8), the current of the anodic peak was higher and the shape of peak was better than that in the other supporting electrolytes. Thus, 0.1M PBS (pH 6.8) was chosen as the supporting electrolyte for further studies.

The electrochemical behaviors of INH in various medium, such as pH=5.0~8.0 phosphate buffer, pH=3.5~5.6 NaAc-HAc buffer, pH=8.0~11.0 NH_3-NH_4Cl buffer, pH=1.8~12. 0 Britton-Robinson buffer (each 0.1mol/L). It is found that the oxidation response of INH was best at pH=6.8 PBS since the peak current was highest and the peak shape was best-defined.

In order to optimize the performance of MIP AuNP-MCNT/GCE, the effect beween loadings of MCNT-Nafion and oxidation current was investigated. The result showed that the peak current increased when the amount of MCNT-Nafion range from 2-4μL, the peak current was almost steady upon further increasing the the amount of MCNT-Nafion. It is disadvantage to electron transfer while the thickness of membrane continues to increase, so 4 μL MCNT/Nafion solution was selected for the experiment.

The effect of the accumulation time on the peak current was also investigated. The result showed that the peak current increased when the accumulation time was less than 60s, and the peak current was almost steady upon further increasing the accumulation time. Here, without loss of generality, in order to ensure the sensitivity and reproducibility, we selected 60s as the accumulation time.

Electrochemistry reduction of AuNP from its ion state contains two competing cathodic processes. One process was the formation of AuNP, and another was the cluster of Au atoms on the surface of gold electrode. In order to enhance the quantity of AuNP, we should improve the formation of AuNP, and supress the cluster. In view of electrodeposition theory, the electrochemical deposition of simple metal ion on the surface of electrode includes 3 steps as follows: (1) The water molecules surrounding metal ions rearrange on the electrode surface liquid layer, lead to empty electronic energy level in the ceter ion up to similar value compared with fermi energy levels on the electrode. (2) The electron transition between electrode and ions, forming the metal atoms (also called absorption atoms) that still were wrapped by hydration layer. (3) When the adsorbed atoms wrapped by hydration layer lose the rest of hydration layer, and become metal atoms located in metal lattice[74]. The results show that the larger of current density and the higher of overpotential, the smaller of nucleation[75], when electrodeposition method was used to prepare AuNP. In addition, the concentration of $HAuCl_4$ had deep influence on the diameter of AuNP, the lower of concentration, the diameter is smaller. The deposite amount and particles' size of AuNP can be controlled by tuning the numbers of scanning cycle. When electrodeposition cycle numbers was few, the catalytical activity was low, and while cycle number was more than 5, the oxidation peak current of INH gradually decrease because of AuNP aggregation. So the cycle numbers was chosen as 5 at the sweep rate of 50mV/s.

The response of INH on MIP-MCNT/GCE and MIP-AuNP-MCNT/GCE

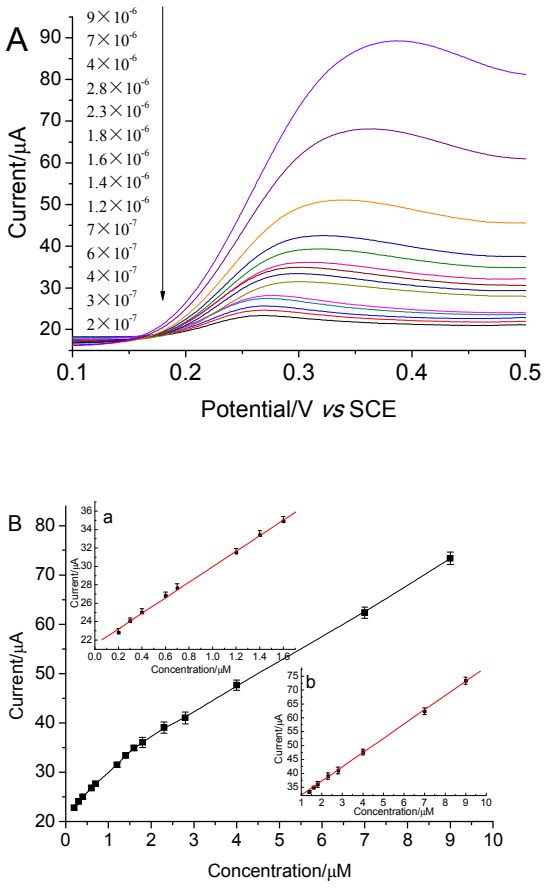

Fig. 7. (A) LSSV responses of MIP MCNT/GCE with different concentration of INH(from 0.2μM to 9μM) in 0.1M PBS. Scan rate is 100 mV/ s. The scan direction is from negative to positive. (B) Calibration curves corresponding to the analysis of INH at MCNT/GCE. Inset(a): Linear detection range from 0.2μM to 1.6μM. Inset (b): Linear detection range from 1.8μM to 10μM.

Linear sweep stripping voltammetry (LSSV) was employed to investigate the response of MIP-MCNT/GCE and MIP-AuNP-MCNT/GCE toward different concentratons of INH. Fig. 7A shows the LSSV response of MIP AuNP-MCNT/GCE with different concentration of INH (from 0.2μM to 9μM) in 0.1M PBS with 50mV/s scan rate. Fig. 7B shows the operating curve of MIP MCNT/GCE in the solution of INH. The linear relation is I(μA) =21.5127+8.4419c (INH, μM) (R=0.9988) while the concentration of INH range from 0.2 to 1.6μM (Fig 7B, inset(a)), and the limit of detection is 0.08μM (S/N=3). As Fig. 7B, inset(b) shows that the MIP MCNT/GCE's linear relation is I(μA) =26.974+5.12828c (INH, μM) (R=0.9997). Fig. 8 shows the working curve of MIP-AuNP–MCNT/GCE toward different concentration of INH. Compared with MIP-MCNT/GCE, the MIP-AuNP-MCNT/GCE show higher sensitivity in the low concentration of INH. On modified electrode of MIP-AuNP-MCNT/GCE, the linear relation between oxidation peak current and the concentration of INH are I(μA)=10.1552+0.178833c (INH, nM) (R=0.9988) and I(μA)=11.6371+0.0933957c (INH, nM) (R=0.9995) while the concentration are 4nM-13nM and 20nM-100nM, respectly. The detection limit is 2 nM (S/N=3). The

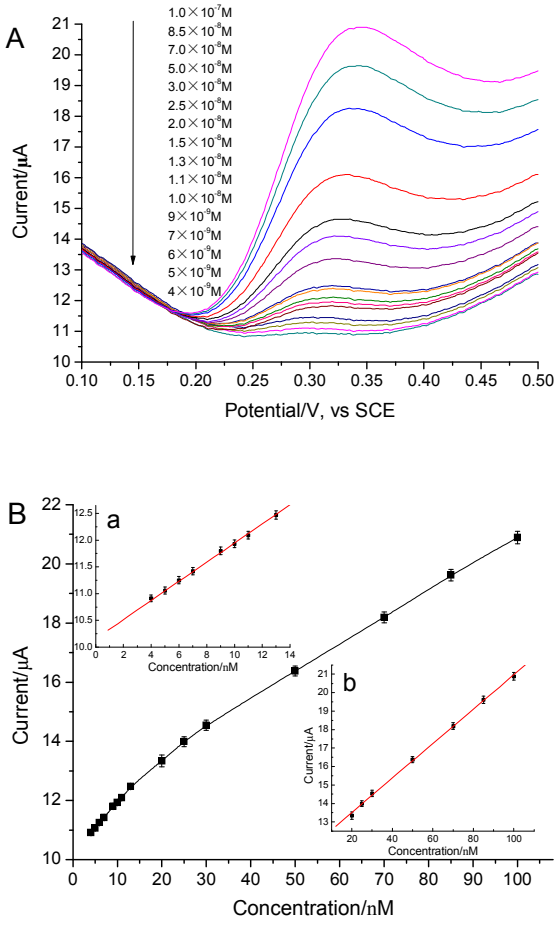

Fig. 8. (A) LSSV responses of MIP AuNP-MCNT/GCE with different concentration of INH (from 4nM to 100nM) in 0.1M PBS. Scan rate is 100 mV/s. The scan direction is from negative to positive. (B) Calibration curves corresponding to the analysis of INH at AuNP-MCNT/GCE. Inset(a): linear detection range from 2nM to 1.4μM. Inset (b): linear detection range from 20nM to 100nM.

above results show that the synergic effect between AuNP and MCNT enhance the sensitivity of the MIP-AuNP-MCNT/GCE.

The functional mechanism of molecular recongnitions were different through the different concentration range, so there were two different slopes. At low concentration, the main effect was ascribe to the hydrogen-bond reaction between INH and the binding site, so the slope of linear range was large. However, when the concentration of INH increasing, there were strong Vander Waals force between INH molecular besides hydrogen bonding adsorption, so the slope of linear relationship was small[76].

Interference

In order to assess the applicability of our sensor, we studied the effect of common components in urine and body fluid. A 0.05μM INH solution, to which interfering species were added, was analyzed. It showed that, with MIP, more than 800-fold excess of K^+, Na^+, Mg^{2+}, Cl^-, 500-fold excess of uric acid, urea, dopamine, glutanic acid, 200-fold excess of starch, glucose, citric acid, $C_2O_4^{2-}$ and 100-fold excess of ascorbic acid, had almost no influence on the LSSV response of 0.05μM INH in PBS (pH 6.8), and the relative error was no larger than 5%. Because the contents of coexisting substancesin urine were all lower than their tolerable concentrations, the proposed sensor could be used to determinate INH directly in urine samples.

The reproducibility test was carried out by 4 MIP–AuNP-MCNT/GCE sensors which were prepared at the same process in 0.05μM INH solution. The relative standard deviation (RSD) for repetitive measurements (6 times) was 4.2%, indicating the reproducibility was good. After the reproducibility test, these sensors were washed in PBS (pH 6.8) and kept for 4 days at room temprature, their peak current and peak potential have no obviously change. Furthermore, surprisingly enough, the peak current still keep more than 95% after 7 days at room temprature, indicating the stability was excellent.

Real sample analysis

The tablet (100 mg per tablet) samples of INH was grinded into the powder and dissolve into water, then diluted with water to 100mL vliumetric flask. The INH was determined by our sensor using the standard addition method. The results were consistent with those obtained by the method in China Pharmacopoeia[77] (see Table 1). The recovery and relative standard deviation (RSD) of INH for the samples were listed in Table 2. the recovery ranges from 96% to 102.5%, and the RSD lower than ± 4.0%.

The results of the INH assay in urine samples by standard recovery tests were shown in Table 3. At the same time, the recoveries of different INH concentration levels varied from 96% to 112%. The result showed that a satisfactory recovery rate could be obtained and that our method was reliable because of the high selectivity of MIP-AuNP–MCNT/GCE.

Conclusions

In this work, a MIP-AuNP–MCNT/GCE electrochemical sensor was constructed. LSSV was employed for determining the content of INH, which has many excellent advantages, such as low detection limit, wide linear range, easy to regenerate, good stability and fast response speed, etc. When the surface of GCE was modified by AuNP-MCNT, making the GCE pocess negative charge and can be viewed as electron donar. The nitrogen atoms in INH molecules can be combined with the surface of AuNP, so the interaction between INH and AuNP can improve the sensitivity of AuNP - MCNT/GCE for detecting low concentrations of analyte INH. That's attribute to the synergistic effect between AuNP and MCNT enhance the electrochemical activity surface area of AuNP–MCNT/GCE. The results demonstrated that the electrochemical sensor not only could strikingly improve the sensitivity and selectivity of INH analysis, but also could obtain good repeatability. And the sensor was low cost, simple and rapid for determining the content in drugs and biological fluid sample.

Table 1. Determination result of isoniazid in tablet (n = 5)

Method	Values (mg/tablet)	RSD(%)
Pharmacopoeia method	100.2	3.9
This method	101.9	3.3
	101.9	1.1
	98.40	1.6

Table 2. Determination result of isoniazid in tablet by standard addition method (n = 3)

Samples	Add (μM)	Founded (μM)	Recovery (%)	RSD (%)
Tablet	0.00	0.15	–	3.0
	0.50	0.66	102.0	2.3
	1.00	1.14	99.00	1.3
	5.00	4.97	96.40	2.8

Table 3. MIP-AuNP–MCNT/GCE applied on determination of INH in blood serum samples ($\times 10^{-6}$M)(n=5)

Added	Found	RSD (%)	Recovery (%)
0.05	0.056	1.04	112.0
0.50	0.48	1.15	96.0
1.50	1.45	1.13	96.7

Our research has shown that the new method can be applied to the detection of INH in pharmaceutical formulations and human urine. So it is a promising candidate for developing new analysis method of INH. The new scheme has many advantages for following reasons: (1) INH can be absorbed selectively on MIP and the special binding property greatly improves the selectivity and sensitivity. (2)Decoration of AuNP on the surface of MCNT leads to the formation of network nano-hybrid (AuNP-MCNT) with attractive electrochemical activities to INH. (3) The MIP -AuNP-MCNT composites system can serve as effective matrixes for fast solid phase extraction target from analytes samples. (4) Desorption of analyte at AuNP-MCNT composites can be readily realized by electrochemical method. (5)It is possible that both extraction and detection can be carried out at the same MIP-AuNP-MCNT composites.

Acknowledgements

This work was supported by the Applied Chemistry Key Subject of Gansu Province (No. GSACKS20130113), the Natural Science Foundation of Gansu Province (No. 1208RJZM289), the Science and Technology Projects of Qingyang (No. KH201302) and the Doctor Foundation of Longdong University (No. XYBY07).

references

1 G. B. Kauffman, *J. Chem. Educ*, 1978, **55**, 448-449.
2 A. S. Yard and H. McKennis, *J. Med. Pharmaceut. Chem.*, 1962, **5**, 196-203.
3 G. K. Mcevory, *AHFS Drug Information*, American Society of Hospital Pharmacists, Bethesda, MD, 1990.
4 K. F. M. Pasqualoto, E. I. Ferreira, O. A. Santos-Filho and A. J. Hopfinger, *J. Med. Chem.*, 2004, **47**, 3755-3764.
5 A. Borba, A. Gómez-Zavaglia and R. Fausto, *J. Phys. Chem. A*, 2009, **113**, 9220-9230.
6 K. Johnsson, D. S. King and P. G. Schultz, *J. Am. Chem. Soc.*, 1995, **117**, 5009-5010.
7 C. Cui, P. Chen and X. Zhao, *J. North Pharm.*, 2014, **11**, 3-5.
8 A. M. El-Brashy and S. M. El-Ashry, *J. Pharm. Biomed. Anal.*, 1992, **10**, 421-426.
9 L. Eidus and A. M. T. Harnanansingh, *Clin. Chem.*, 1971, **17**, 492-494.
10 B. Zargar and A. Hatamie, *Spectrochim. Acta. A. Mol. Biomol. Spectrosc.*, 2013, **106**, 185-189.
11 L. Lahuerta Zamora, J. V. Garcia Mateo and J. Martinez Calatayud, *Anal. Chim. Acta*, 1992, **265**, 81-86.
12 R. A. S. Lapa, J. L. F. C. Lima and J. L. M. Santos, *Anal. Chim. Acta*, 2000, **419**, 17-23.
13 P. C. Ioannou, *Clin. Chim. Acta*, 1988, **175**, 175-181.
14 M. Lever, *Biochem. Med.*, 1972, **6**, 65-71.
15 P.-F. Fang, H.-L. Cai, H.-D. Li, R.-H. Zhu, Q.-Y. Tan, W. Gao, P. Xu, Y.-P. Liu, W.-Y. Zhang, Y.-C. Chen and F. Zhang, *J. Chromatogr. B*, 2010, **878**, 2286-2291.
16 Z.-m. Zhou, D.-y. Zhao, J. Wang, W.-j. Zhao and M.-m. Yang, *J. Chromatogr. A*, 2009, **1216**, 30-35.
17 H. I. Seifart, W. L. Gent, D. P. Parkin, P. P. van Jaarsveld and P. R. Donald, *J. Chromatogr. B. Biomed. Appl.*, 1995, **674**, 269-275.
18 P. Liu, Z. Fu, J. Jiang, L. Yuan and Z. Lin, *Biomed. Chromatogr.*, 2013, **27**, 1150-1156.
19 Y. Liu, Z. Fu and L. Wang, *Luminescence*, 2010, **26**, 397–402.
20 J. Liu, W. Zhou, T. You, F. Li, E. Wang and S. Dong, *Anal. Chem.*, 1996, **68**, 3350-3353.
21 M. Khuhawar and L. Zardari, *J. Food Drug Anal.*, 2006, **14**, 323-328.
22 B. Haghighi and S. Bozorgzadeh, *Microchem. J.*, 2010, **95**, 192-197.
23 A. Safavi, M. A. Karimi and M. R. H. Nezhad, *J. Pharm. Biomed. Anal.*, 2003, **30**, 1499-1506.
24 S. Zhang and H. Li, *Anal. Chim. Acta*, 2001, **444**, 287-294.
25 S. A. Halvatzis, M. M. Timotheou-Potamia and A. C. Calokerinos, *Analyst*, 1990, **115**, 1229-1234.

26 B. Wu, Z. Wang, z. Xue, X. Zhou, J. Du, X. Liu and X. Lu, *Analyst*, 2012, **137**, 3644-3652.
27 L. Liu, X. Zheng and Z. Zhang, *Chin. J. Anal. Chem.*, 2003, **32**, 1112-1114.
28 A. Espinosa-Mansilla, M. I. Acedo Valenzuela, A. Muñoz de la Peña, F. Salinas and F. C. Cañada, *Anal. Chim. Acta*, 2001, **427**, 129-136.
29 K. Asadpour-Zeynali and P. Soheili-Azad, *Electrochim. Acta*, 2010, **55**, 6570-6576.
30 M. F. Bergamini, D. P. Santos and M. V. B. Zanoni, *Bioelectrochemistry*, 2010, **77**, 133-138.
31 S. Shahrokhian and M. Amiri, *Microchim. Acta*, 2007, **157**, 149-158.
32 M. R. Majidi, A. Jouyban and K. Asadpour-Zeynali, *J. Electroanal. Chem.*, 2006, **589**, 32-37.
33 J. Tong, X.-J. Dang and H.-L. Li, *Electroanal.*, 1997, **9**, 165-168.
34 U. P. Azad, N. Prajapati and V. Ganesan, *Bioelectrochemistry*, 2015, **101**, 120-125.
35 M. Satyanarayana, K. K. Reddy and K. V. Gobi, *Anal. Methods*, 2014, **6**, 3772-3778.
36 S. Cheemalapati, S. M. Chen, M. A. Ali and F. M. Al-Hemaid, *Colloids and Surfaces B: Biointerfaces*, 2014, **121**, 444-450.
37 H. Yan, H. Xiao, Q. Xie, J. Liu, L. Sun, Y. Zhou, Y. Zhang, L. Chao, C. Chen and S. Yao, *Sens. Actuators, B*, 2015, **207, Part A**, 167-176.
38 X. Si, L. Jiang, X. Wang, Y. Ding and L. Luo, *Anal. Methods*, 2015, **7**, 793-798.
39 S. Iijima, *Nature*, 1991, **354**, 56-58.
40 B. J. Privett, J. H. Shin and M. H. Schoenfisch, *Anal. Chem.*, 2010, **82**, 4723-4741.
41 C. B. Jacobs, M. J. Peairs and B. J. Venton, *Anal. Chim. Acta*, 2010, **662**, 105-127.
42 V. K. Gupta, M. L. Yola, N. Atar, Z. Ustundağ and A. O. Solak, *Electrochim. Acta*, 2013, **112**, 541-548.
43 H. Karimi-Maleh, F. Tahernejad-Javazmi, N. Atar, M. L. Yola, V. K. Gupta and A. A. Ensafi, *Ind. Eng. Chem. Res.*, 2015, **54**, 3634-3639.
44 F. Golestanifar, H. Karimi-Maleh, N. Atar, E. Aydogdu, B. Ertan, M. Taghavi, M. L. Yola and M. Ghaemy, *Int. J. Electron.Sci.*, 2015, **10**, 5456-5464.
45 A. N. Shipway, E. Katz and I. Willner, *Chemphyschem*, 2000, **1**, 18-52.
46 R. N. Goyal, V. K. Gupta, M. Oyama and N. Bachheti, *Electrochem. Commun.*, 2005, **7**, 803-807.
47 M. L. Yola, T. Eren and N. Atar, *Electrochim. Acta*, 2014, **125**, 38-47.
48 V. K. Gupta, M. L. Yola, M. S. Qureshi, A. O. Solak, N. Atar and Z. Üstündağ, *Sens. Actuators, B*, 2013, **188**, 1201-1211.
49 S. Guo and S. Dong, *TrAC, Trends Anal. Chem.*, 2009, **28**, 96-109.
50 Y. Guo, S. Guo, Y. Fang and S. Dong, *Electrochim. Acta*, 2010, **55**, 3927-3931.
51 F. Valentini, A. Amine, S. Orlanducci, M. L. Terranova and G. Palleschi, *Anal. Chem.*, 2003, **75**, 5413-5421.
52 B. Wu, L. Hou, M. Du, T. Zhang, Z. Wang, Z. Xue and X. Lu, *RSC Advances*, 2014, **4**, 53701-53710.
53 M. L. Yola and N. Atar, *Electrochim. Acta*, 2014, **119**, 24-31.
54 N. Atar, T. Eren, M. L. Yola, H. Karimi-Maleh and B. Demirdogen, *RSC Advances*, 2015, **5**, 26402-26409.
55 V. K. Gupta, M. L. Yola, N. Özaltın, N. Atar, Z. Üstündağ and L. Uzun, *Electrochim. Acta*, 2013, **112**, 37-43.
56 M. L. Yola, N. Atar and T. Eren, *Sens. Actuators, B*, 2014, **198**, 70-76.
57 M. L. Yola, T. Eren and N. Atar, *Sens. Actuators, B*, 2015, **210**, 149-157.
58 M. L. Yola, T. Eren and N. Atar, *Biosens. Bioelectron.*, 2014, **60**, 277-285.
59 V. K. Gupta, M. L. Yola and N. Atar, *Sens. Actuators, B*, 2014, **194**, 79-85.
60 T. Eren, N. Atar, M. L. Yola and H. Karimi-Maleh, *Food Chem.*, 2015, **185**, 430-436.
61 V. K. Gupta, M. L. Yola, T. Eren and N. Atar, *Sens. Actuators, B*, 2015, **218**, 215-221.
62 M. L. Yola, L. Uzun, N. Özaltın and A. Denizli, *Talanta*, 2014, **120**, 318-324.
63 M. L. Yola, T. Eren and N. Atar, *Sens. Actuators, B*, 2014, **195**, 28-35.
64 N. Atar, T. Eren and M. L. Yola, *Food Chem.*, 2015, **184**, 7-11.
65 N. Atar, T. Eren, M. L. Yola and S. Wang, *Sens. Actuators, B*, 2015, **216**, 638-644.
66 W. Zhihua, C. Yiwen, Z. Huini, L. Xiaoning and K. Jingwall, *Chemical Research And Application*, 2009, **21**, 1370-1374.
67 L. Mao, R. Yuan, Y. Chai, Y. Zhuo, X. Yang and S. Yuan, *Talanta*, 2010, **80**, 1692-1697.
68 M. Zhang, K. Gong, H. Zhang and L. Mao, *Biosens. Bioelectron.*, 2005, **20**, 1270-1276.
69 M. J. Moghaddam, S. Taylor, M. Gao, S. Huang, L. Dai and M. J. McCall, *Nano Lett.*, 2004, **4**, 89-93.
70 Y. Liu, X. Qu, H. Guo, H. Chen, B. Liu and S. Dong, *Biosens. Bioelectron.*, 2006, **21**, 2195-2201.
71 H. O. Finklea, D. A. Snider, J. Fedyk, E. Sabatani, Y. Gafni and I. Rubinstein, *Langmuir*, 1993, **9**, 3660-3667.
72 N. Chauhan and C. S. Pundir, *Anal. Biochem.*, 2011, **413**, 97-103.
73 E. Hammam, A. M. Beltagi and M. M. Ghoneim, *Microchem. J.*, 2004, **77**, 53-62.
74 Q. Zha, *Introduction kinetics of electrode process (3rd Edition)*, Science Press, Beijing, 2002.
75 M. T. Reetz and W. Helbig, *J. Am. Chem. Soc.*, 1994, **116**, 7401-7402.
76 Z. Wang, H. Li, J. Chen, Z. Xue, B. Wu and X. Lu, *Talanta*, 2011, **85**, 1672-1679.
77 *The Pharmacopoeia Committee of the Ministry of Health of PR China, Pharmacopoeia of PR China Part II*, Chemical Industry Press, Beijing, 2005.

Graphical Abstract

In this work, we introduce a novel molecularly imprinted electrochemical sensor to determine isoniazid (INH) with functionalization nanocomposites based on molecular imprinting and electrochemical technology. The imprinted electrode could avoid interference successfully. The oxidation peak current and INH concentration have linear relationship in range of 1×10^{-9} to 1.4×10^{-8} M and 2×10^{-8} to 1.0×10^{-7} M, resepectively. The detection limit is 0.3×10^{-9}M (3σ) INH with relative standard deviation 4.6% (n=8) for 5×10^{-8}M INH after 60s enrichment. The sensor exhibits remarkable advantages, such as higher sensitivity, wider linear range and lower detection limit. The effective method has a potential application to monitor INH in body fluid and pharmaceutical samples selectively.